JOURNAL OF THE MECHANICAL BEHAVIOR OF BIOMEDICAL MATERIALS ▮ (▮▮▮▮) ▮▮▮–▮▮▮

Available online at www.sciencedirect.com

SciVerse ScienceDirect

www.elsevier.com/locate/jmbbm

Research Paper

The weak interfaces within tough natural composites: Experiments on three types of nacre

*Ahmad Khayer Dastjerdi, Reza Rabiei, Francois Barthelat**

Department of Mechanical Engineering, McGill University, 817 Sherbrooke Street West, Montreal, QC, Canada H3A 2K6

ARTICLE INFO

Article history:
Received 8 May 2012
Received in revised form
5 September 2012
Accepted 7 September 2012

Keywords:
Nacre
Organic interface
Interfacial fracture toughness
Chevron notch fracture test
Fractography

ABSTRACT

Mineralization is a typical strategy used in natural materials to achieve high stiffness and hardness for structural functions such as skeletal support, protection or predation. High mineral content generally leads to brittleness, yet natural materials such as bone, mollusk shells or glass sponge achieve relatively high toughness considering the weakness of their constituents through intricate microstructures. In particular, nanometers thick organic interfaces organized in micro-architectures play a key role in providing toughness by various processes including crack deflection, crack bridging or energy dissipation. While these interfaces are critical in these materials, their composition, structure and mechanics is often poorly understood. In this work we focus on nacre, one of the most impressive hard biological materials in terms of toughness. We performed interfacial fracture tests on chevron notched nacre samples from three different species: red abalone, top shell and pearl oyster. We found that the intrinsic toughness of the interfaces is indeed found to be extremely low, in the order of the toughness of the mineral inclusions themselves. Such low toughness is required for the cracks to follow the interfaces, and to deflect and circumvent the mineral tablets. This result highlights the efficacy of toughening mechanisms in natural materials, turning low-toughness inclusions and interfaces into high-performance composites. We found that top shell nacre displayed the highest interfacial toughness, because of higher surface roughness and a more resilient organic material, and also through extrinsic toughening mechanisms including crack deflection, crack bridging and process zone. In the context of biomimetics, the main implication of this finding is that the interface in nacre-like composite does not need to be tough; the extensibility or ductility of the interfaces may be more important than their strength and toughness to produce toughness at the macroscale.

1. Introduction

A large number of materials in nature are mineralized in order to properly fulfill their functions. For example bone, seashells or teeth contain large amounts of minerals (varying from about 30 to 70 vol% in bone to 95% in seashells) which are required for high stiffness and hardness. In the most extreme cases where hardness is critical, tissue can contain up to 99 vol% mineral (tooth enamel, and sea urchin spines). The structure and mechanics of these hard biological tissues have been of great interest to material scientists over the past two decades because of their remarkable mechanical performance (Wang and Gupta, 2011; Launey et al., 2010; Imbeni et al., 2005, Espinosa et al., 2009; Barthelat et al., 2007a).

*Corresponding author.
E-mail address: francois.barthelat@mcgill.ca (F. Barthelat).

1751-6161/$ - see front matter © 2012 Elsevier Ltd. All rights reserved.
http://dx.doi.org/10.1016/j.jmbbm.2012.09.004

Despite high contents of brittle minerals, these materials exhibit outstanding strength and toughness originating from the way these ingredients are combined into intricate architectures (Barthelat et al., 2007a; Launey et al., 2010). The mineral phase itself comes in the form of micro- or nano-size layers, rods, grains or platelets bonded by soft organic materials (proteins and in some cases, polysaccharides). The mineral provides stiffness but it is brittle and linear elastic, so that it is the interfaces which provide energy dissipation (nacre, bone (Fratzl et al., 2004; Fratzl, 2007; Dastjerdi et al., 2012; Fantner et al., 2006, Smith et al., 1999a; Hansma, 2005)), control crack deflection (glass sponge spicules (Sarikaya et al., 2001; Mayer and Sarikaya, 2002), conch shell (Kuhn-Spearing et al., 1996)), or guide cracks towards regions of the material where they become trapped (as in tooth enamel (Imbeni et al., 2005)). Despite the central role of these interfaces in high performance natural materials, too often little is known on their composition, structure and properties. Nacre is one of these materials controlled by interface mechanics. Nacre is the iridescent layer found inside the shell of many mollusk species, and it has attracted a great deal of attention for biomimetic purposes owing to its high performance and robust, albeit relatively simple structure (Barthelat, 2007; Barthelat and Zhu, 2011; Deville et al., 2006; Munch et al., 2008). Nacre is composed of about 95 vol% brittle aragonite (one of the crystalline forms of calcium carbonate), and of about 5% organic material (a compound of proteins and polysaccharides) (Sarikaya and Aksay, 1995). The microstructure of nacre resembles a brick-wall, where 0.2–0.9 μm thick aragonite tablets are cemented together by means of thin 30 nm organic layers serving as "mortar" (Fig. 1) (Currey, 1977). The staggered arrangement of the tablets in nacre is a remarkable design feature which provides the structure with outstanding combination of stiffness, strength and toughness (Jäger and Fratzl, 2000; Rabiei et al., 2010; Gao, 2006; Jackson et al., 1988).

Under tension, the tensile stress in tablets is transferred to the neighboring platelets through the soft interfaces enclosing the tablet (Jäger and Fratzl, 2000; Kotha et al., 2001). Since the tablets in nacre are essentially brittle and linear elastic, the toughness and energy absorption capability of the structure stems from mechanisms working at the interface (Fratzl et al., 2004) including inelastic shear deformation of the organic phase (Smith et al., 1999b), interlocking of nano-asperities (Wang et al., 2001) and microscale waviness (Barthelat et al., 2007a), and fracture of mineral bridges (Song and Bai, 2003). Several models have so far been proposed for the structure of the organic polymers (Schäffer et al., 1997; Blank et al., 2003; Weiner et al., 1984), but the most widely accepted model consists of three layers where a stiff core of fibrous chitin is sandwiched between two proteinic sheets (Schäffer et al., 1997). The organic materials are strongly bonded onto the mineral tablets, and in fact they extend into the mineral tablets in the form of a fine network organized around mineral nanograins (Blank et al., 2003; Rousseau et al., 2005). Single-molecule force spectroscopy on freshly cleaved interfaces using atomic force microscopy (AFM) showed how the organic layer dissipates energy through unfolding of macromolecules and rupture of sacrificial bonds, a process which is reversible and repeatable (Smith et al., 1999a). The properties of the organic layers were also recently investigated by Meyers et al. (2009) who used nanoindentation techniques to deflect thin organic membranes. Their findings suggest that while the organic phase at the interface is essential to the growth of the shell by means of subdividing the mineral phase into thin platelets, it may not have a significant role in providing mechanical strength (Meyers et al., 2008). A more recent AFM study has shown that biopolymers connecting two adjacent aragonite tablets in nacre exhibit strain hardening in tension, which can translate into higher strength and toughness for nacre (Xu and Li, 2011). Bezares et al. (2010) have also recently investigated the constitutive properties of organic matrix from red abalone nacre by using tensile and time dependent relaxation tests on demineralized samples. They demonstrate that the organic framework essentially follows a viscoelastic behavior mainly governed by the chitin core of the matrix. The properties of the matrix were also evaluated by indirect means. For example, the shear strength of the organic interface was evaluated from simple shear tests on whole nacre samples (25 MPa (Barthelat et al., 2007a)), while the maximum elongation was evaluated from imaging (600 nm (Barthelat et al., 2007a)). Combining this data led to the cohesive law of the interface, which represents the traction across the interface as function of opening and/or sliding. In turn, the area under the cohesive law can be used to evaluate toughness, which gives a value of about 10 J/m^2 (Barthelat et al., 2007a). This value is surprisingly low, and contrasts with a common perception of the nacreous proteins as a tough adhesives. For comparison, the estimated toughness of nacreous interfaces is only five times higher than a typical office tape on glass (2 J/m^2, measured from peel tests (Dastjerdi et al., 2012)). With these

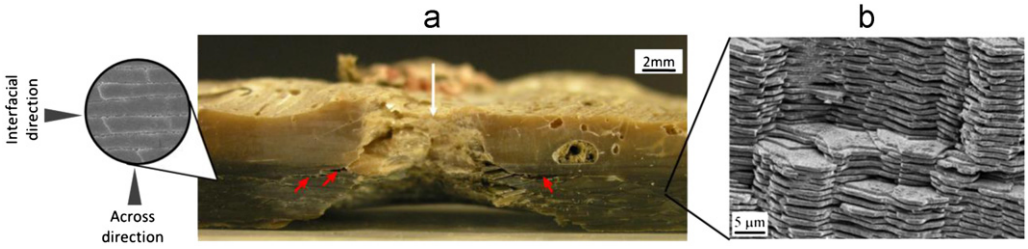

Fig. 1 – (a) Cross section of a punctured red abalone shell (Yourdkhani et al., 2011). Red and white arrows in the picture indicate the cracks deflected through the interface of the tablets and the puncture direction, respectively and (b) SEM micrograph showing the brick and mortar microstructure of nacre. (For interpretation of the references to colour in this figure legend, the reader is referred to the web version of this article.)

Please cite this article as: Khayer Dastjerdi, A., et al., The weak interfaces within tough natural composites: Experiments on three types of nacre. Journal of the Mechanical Behavior of Biomedical Materials (2012), http://dx.doi.org/10.1016/j.jmbbm.2012.09.004

estimates in mind, one can appreciate the powerful toughening mechanisms that must operate in nacre to yield its remarkable macroscopic toughness. Another dimension of complexity is the variation of structure, mechanics and toughness across nacres from different mollusk species (Wang et al., 2001; Currey, 1977). For example, recent fracture experiments showed that nacre from pearl oyster is almost three times tougher than nacre from red abalone in the direction across the layers (Rabiei et al., 2010). Whether this difference should be attributed to the differences in the properties of the organic materials or to the differences in the efficiencies of toughening mechanisms is not known. Direct measurements of the toughness of these interfaces are lacking, and may answer these questions. In turn, a better understanding of the fracture of nacre will facilitate the development of successful biomimetic composites (Espinosa et al., 2009; Barthelat, 2007).

Currey (1977) was the first to perform fracture tests on nacre along the direction of the tablets in order to measure the toughness of the interface. He found that the work of fracture in the interfacial direction is about ten times lower than that in the across direction for nacre from pearl oyster (*Pinctada margaritifera*). While these findings were useful, work of fracture (energy required to fracture a notch specimen divided by the surface area of the fracture surface) may overestimate the actual toughness of the interface if the crack is unstable because a large portion of the energy measured through this method may be consumed in dynamic effects such as crack acceleration (Barinov, 1993). Recent experiments on whole shells also showed that delamination cracks can occur in the nacreous layer during penetration (Fig. 1b (Yourdkhani et al., 2011)). Understanding the structure and properties of these nanometers-thick interfaces is therefore of utmost importance in the context of biomimetics.

2. Interfacial fracture toughness

The interfacial fracture resistance of nacre from red abalone, black-lip pearl oyster, and top shell was characterized in this work. This selection was motivated by previous work which characterized and measured the fracture toughness of these three types of nacre in the fracture direction across the tablets (Rabiei et al., 2010). Fracture specimens were prepared by harvesting approximately $9 \times 5\ mm^2$ plates from the nacreous layer of the shells using a precision diamond saw. The average specimen thickness was 2.7 mm for red abalone, 3.7 mm for pearl oyster and 4.3 mm for top shell (samples displayed variations in dimensions because of limitations due to the shell thickness). A 60° chevron notch was then cut into the specimens using a diamond saw (Fig. 2). The chevron geometry was used because it promotes stable crack propagation, and because it does not require the initial notch to be perfectly sharp. Opening forces were exerted through two steel tubes glued onto the ends of the specimen using cyanoacrylate glue (Fig. 2). Finally, the diamond saw notch was sharpened using a fresh razor blade. To perform the test, the specimen was placed in a horizontal miniature loading stage (Ernest F. Fullam, Inc., Latham, NY) equipped with two vertical pins in order to impose displacements on the two steel tubes. A fixed displacement rate of 3 μm/s was applied to all the tests, while the load was recorded with a 110 N load cell. All the specimens were kept in hydrated condition before and throughout the experiments.

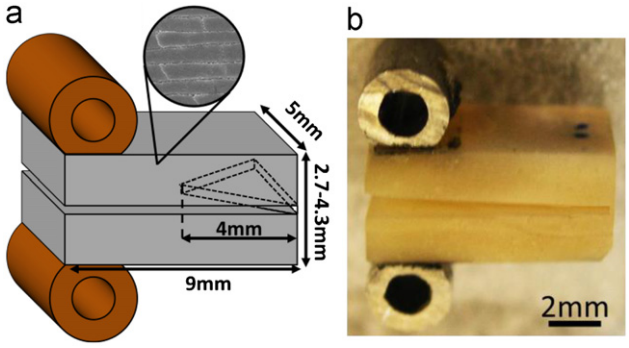

Fig. 2 – (a) Schematic of the chevron notch specimen with dimensions and (b) an actual image of a specimen made from top shell nacre.

Fig. 3a shows three typical load–displacement curves obtained for each type of nacre. All specimens initially displayed a linear response followed by a nonlinear regime indicating stable crack propagation (marked by arrows in Fig. 3a). The samples displayed significant differences in initial stiffness because of variations in the thickness of the specimens (stiffness scales with the thickness cubed). The nonlinear response of red abalone nacre was short and the specimens rapidly failed in a brittle fashion. In contrast, nacre from top shell and pearl oyster displayed relatively stable interfacial crack propagation and a longer nonlinear region on the load–displacement curves. A work of fracture may be computed from this data, by dividing the area under the load–displacement curve by the surface area of the fractured surface. However this measurement may overestimate the actual energy required to fracture the interface, since a large portion of the measured energy may be consumed in dynamic effects including crack acceleration (Buehler and Xu, 2010). For example, the apparent work of fracture on top shell is about $500\ J/m^2$, an unrealistically high value considering that the work of fracture in the across direction, where the structure is much more difficult to fracture, is about $700\ J/m^2$ (Rabiei et al., 2010).

Instead of using work of fracture, the interfacial fracture toughness was calculated from the maximum load F_{max} and the geometry and elastic properties of the chevron notch specimens using:

$$J_{IC} = F_{max}^2 \left(\frac{1}{2w(a)} \frac{\partial C}{\partial a} \right)_{min} = F_{max}^2 I_{min}. \quad (1)$$

In this equation C and w denote the compliance and width of the specimen at crack length a. In this work I_{min} was determined numerically, from a three-dimensional model of the chevron specimens built using the commercial finite element software ABAQUS (v. 6.9, ABAQUS Inc., Providence, RI). The specimens were modeled as a transversely isotropic material ($E_z = 30$ GPa, $E_p = 70$ GPa, $G_{zp} = 10$ GPa, and $\upsilon_p = \upsilon_{zp} = 0.2$ (Barthelat, 2006)) with plane of isotropy being parallel to the fracture surface of the specimens. Appropriate boundary

Please cite this article as: Khayer Dastjerdi, A., et al., The weak interfaces within tough natural composites: Experiments on three types of nacre. Journal of the Mechanical Behavior of Biomedical Materials (2012), http://dx.doi.org/10.1016/j.jmbbm.2012.09.004

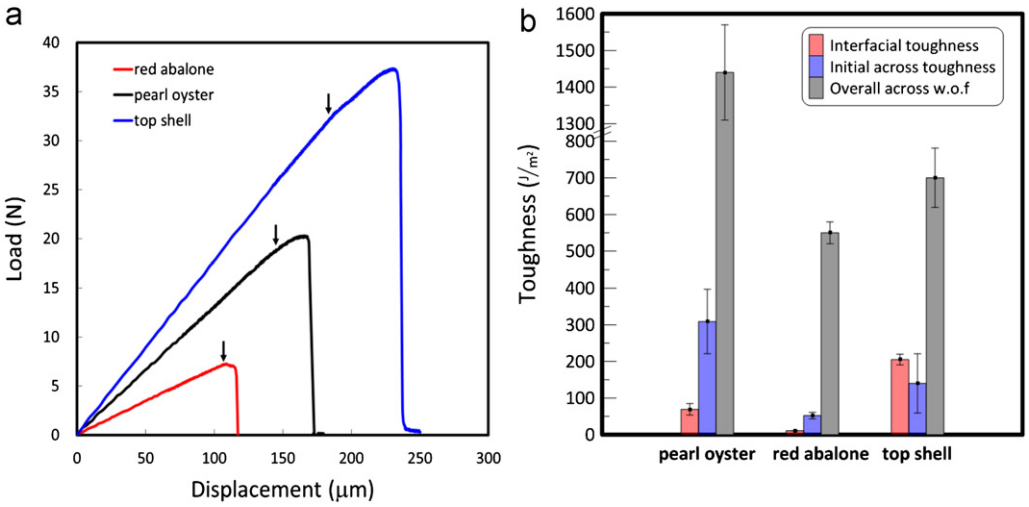

Fig. 3 – (a) Typical load–displacement curves of the different shells obtained from chevron notch test. Arrows indicate the onset of crack propagation in each specimen; (b) interfacial fracture toughness (average and standard deviation). The across fracture toughness is also shown (data from Rabiei et al., 2010).

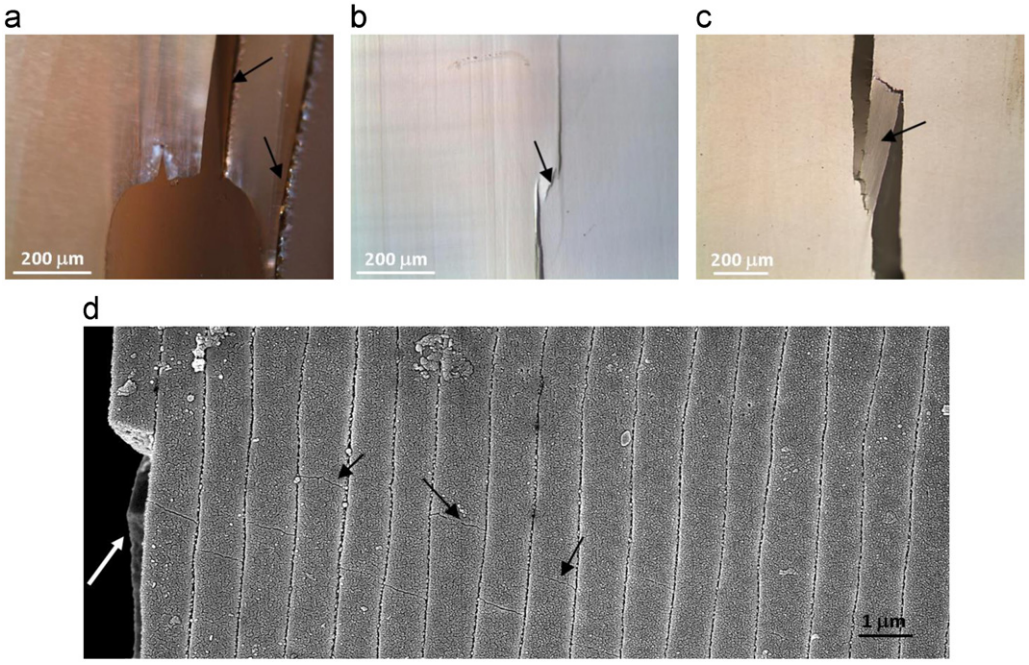

Fig. 4 – In-situ optical images taken from (a) red abalone, (b) pearl oyster, and (c) top shell. Black arrows in (a) indicate the growth line, and in (b) and (c) show un-cracked ligament bridges. (d) SEM micrograph of the top shell specimen showing junction opening (black arrows) at an area close to the crack wall (white arrow).

conditions were applied along the two symmetry planes of the model, and the compliance of the system was determined at different crack lengths. I_{min} was then determined for each sample geometry. Finally, the interfacial toughness of the specimens was determined using Eq. (1), yielding $J_{IC}=205\pm14\,J/m^2$ for top shell, $J_{IC}=69\pm16\,J/m^2$ for pearl oyster, and $J_{IC}=11\pm1\,J/m^2$ for red abalone. These results are reported in Fig. 3b, where for comparison purposes the "across" fracture toughness (crack propagation across the direction of the tablets) is also included (the values taken from previous fracture tests (Rabiei et al., 2010)). Since across fracture produces a rising crack-resistance curve where toughness increases as crack advances, both the initial toughness (upon initiation of crack propagation) and the maximum toughness (about 5–10 times higher because of bridging and process zone toughening (Barthelat and Rabiei, 2011)) are reported for the across direction. Interfacial toughness is lower than across work of fracture, because it is generally much easier for the crack to propagate along the interfaces (the same observations were made on cortical bone (Koester et al., 2008)). For pearl oyster and red abalone, we found that the interfacial toughness is lower than the

Please cite this article as: Khayer Dastjerdi, A., et al., The weak interfaces within tough natural composites: Experiments on three types of nacre. Journal of the Mechanical Behavior of Biomedical Materials (2012), http://dx.doi.org/10.1016/j.jmbbm.2012.09.004

initial toughness upon crack initiation in the across case. This is expected because at the onset of across crack propagation the pullout of tablets and the shearing of the interfaces produce more toughness than mode I fracture of straight interfaces. Crack bridging has been shown to amplify the toughness of the interfaces and provide the initial toughness for staggered composites like nacre (Barthelat and Rabiei, 2011). The results we obtained on top shell however contradict this trend. The interfacial toughness was found to be significantly higher than that of other types of nacre, and slightly higher than the initial toughness value in the across direction. This suggests tougher interfaces and toughening mechanisms operating in top shell even in the interfacial direction.

A second set of experiments were therefore performed on "half chevron" specimens in order to observe interfacial crack propagation in-situ and investigate potential toughening mechanisms in the interfacial mode. The "half chevron" notch specimens were prepared by cutting chevron specimens across their width and along the longitudinal direction. The geometry obtained is therefore a "half-chevron" which still promotes stable crack propagation but with an exposed side which was polished down to 0.05 μm particle size for imaging of the crack. The fracture experiments were performed under an optical microscope (BX-51M, Olympus, Markham, Canada) equipped with a CCD camera (RETIGA 2000R, Qimaging, Surrey, Canada) to acquire images with a 300-μs time interval during crack propagation. Fig. 4 displays some of the optical images taken from the polished surface of the specimens during the crack growth along the tablets interfaces. In red abalone nacre, the crack invariably followed a growth line despite the presence of a sharp razor blade notch (Fig. 4a). Growth lines are ~20 μm thick layers of organic material (Erasmus, 1994; Lin and Meyers, 2005) believed to form during periods in which mineral growth lessens due to an interruption in feeding (Lin and Meyers, 2005), and which represent extremely weak interfaces. This could therefore explain why the interfacial fracture toughness of red abalone is significantly lower than that of pearl oyster and top shell, which do not contain any growth lines.

Cracking in pearl oyster and top shell followed the interfaces between the tablets, with evidence of crack deflection (Figs. 4b and c) and un-cracked ligament bridges. Un-cracked ligament bridging is a powerful toughening mechanism observed in a wide range of materials including bone, dentine, metals and composites (Ritchie, 1999; Nalla et al., 2003; Kruzic et al., 2003). In addition, in top shell a diffuse white "process zone" was observed ahead of the crack tip and on both sides of the crack. Stress whitening, a well-documented phenomenon in nacre and bone (Zioupos et al., 2008; Rabiei et al., 2010; Thurner, 2007), is an optical indication of tablet separation due to inelastic sliding and junction opening. This is, however, the first time that a process zone is observed in nacre during interfacial fracture. Fig. 4d presents an SEM micrograph of a crack wall from a polished fracture sample of top shell where openings of the tablets (i.e. inelastic deformation) are visible. The size of the process zone measured from this type of image is about 10 μm, which is almost 40 times smaller than the measured size of the process zone in the across direction (Rabiei et al., 2010). The apparent interfacial fracture toughness measured from these chevron tests includes all the toughening mechanisms discussed above, making it impossible to directly measure the intrinsic toughness of the interfaces. However, an estimate of the toughness can be obtained from the analysis of the process zone size. Ahead of the crack tip biaxial tension dominates, and tablet sliding may be initiated if the tensile stress along the tablets reaches the tensile strength of the structure in this direction (σ_S). The asymptotic stress field can then be related to the size of the inelastic region (r_i) (Anderson, 1995):

$$\sigma_{xx} = \frac{K_{IC}}{\sqrt{2\pi r_i}} \cos\left(\frac{\theta}{2}\right)\left[1-\sin\left(\frac{\theta}{2}\right)\sin\left(\frac{3\theta}{2}\right)\right]. \quad (2)$$

Knowing that the maximum height of inelastic region occurs at an angle $\theta=30^\circ$ from the crack line leads to the simple expression:

$$K_{IC} = \frac{2\sqrt{\pi h}}{0.79}\sigma_S \quad (3)$$

where $h(=r_i \sin(\theta))$ is the maximum width of the process zone. Using $\sigma_S=60$ MPa (Barthelat et al., 2007b) and $h=10$ μm (measured from the SEM imaging, Fig. 4d) leads to $K_{IC}=0.43$ MPa $m^{1/2}$. This toughness can be converted to an energy form using $J_{IC}=(1-\upsilon^2)K_{IC}^2/E$ for plane strain condition, where $E=30$ GPa (Barthelat et al., 2007b) is the elastic modulus of nacre across the direction of the tablets. This calculation leads to a value of $J_{IC}=5.5$ J/m^2 for the intrinsic plus process zone toughness of the interface. In pearl oyster and red abalone, the fact that no process zone larger than a few tablet widths was observed implies a maximum higher bound of approximately 1 J/m^2 for the intrinsic toughness of the organic interface. These estimations are slightly lower than previous estimates from the interfacial cohesive law reported in Barthelat et al. (2007a), possibly toughening mechanisms operating during the tests used to calibrate the cohesive law "masked" the actual intrinsic toughness of the interfaces. The intrinsic toughness of the interface is therefore extremely low and in the order of the toughness of office tape on glass. Powerful toughening mechanisms such as sacrificial bonds probably contribute greatly to the intrinsic toughness (Smith et al., 1999a), but the nano-confinement of these proteins is so severe that the contribution of toughening mechanisms associated with volumetric energy dissipation remain small. This effect is similar to ductile adhesive joint, which display lower apparent toughness for thinner bond lines because the plastic region cannot form fully (Tvergaard and Hutchinson, 1996). Surprisingly the toughness of the interfaces is also comparable to the toughness of the mineral tablets in terms of critical stress intensity ($K_{IC}=0.39$ MPa $m^{1/2}$ for calcite (Broz et al., 2006) and $K_{IC}=0.43$ MPa $m^{1/2}$ for interfaces), as well as in energy terms ($J_{IC}=1.8$ J/m^2 for calcite and $J_{IC}=1$–5.5 J/m^2 for the interfaces). In terms of mechanics, low interfacial toughness is required to promote crack deflection when nacre fractures across the tablets (Ming-Yuan and Hutchinson, 1989). This underlines the efficacy of powerful bridging and process zone toughening mechanisms which "amplify" the toughness of both mineral inclusions and interfaces (Barthelat and Rabiei, 2011) to produce a tremendous toughness at the macroscale.

Please cite this article as: Khayer Dastjerdi, A., et al., The weak interfaces within tough natural composites: Experiments on three types of nacre. Journal of the Mechanical Behavior of Biomedical Materials (2012), http://dx.doi.org/10.1016/j.jmbbm.2012.09.004

3. Fractography

The fracture processes and toughening mechanisms in the three different types of nacre can be unveiled by examination of the fracture surfaces. The fracture surface of the specimens was coated with a 20 nm conductive Au–Pd layer and examined using a scanning electron microscope (FEG-SEM, Hitachi S-4700, Japan). Fig. 5 shows typical fracture surfaces for each type of nacre tested at different magnifications. These images were collected near the apex of the chevron region where crack propagation was stable. For all samples the crack predominantly propagated along the interfaces of the tablets, but each type of nacre showed distinct fracture characteristics. In red abalone, the crack deflected and propagated through the weaker growth lines present in the material (Lin and Meyers, 2005) (Figs. 5a and 7d). In pearl oyster, cracks underwent less deflection, leading to an overall smoother fracture surface compared to red abalone (Fig. 5b). Finally the fracture surface of top shell did not display any apparent sign of major crack deflection at low magnification (Fig. 5c), but higher magnifications revealed a continuous stair-like deflection pattern (Fig. 5f). SEM imaging of pearl oyster also revealed broken tablets in all three nacres. An example of tablet failure is shown in Fig. 5e for pearl oyster where distinct ridges are evident, which suggest a brittle, unstable fracture of the tablets (Buehler and Xu, 2010).

The fracture surfaces were also examined at higher magnification using an atomic force microscopy (AFM, Veeco Dimension V, Santa Barbara, CA). The organic material was removed from the surface using plasma etching. Fig. 5g–i show height AFM images of the nanoasperies on the surface of the tablets. The nanograins appeared elongated and larger in tablets from top shell and red abalone while smaller and more uniformly distributed in tablets from pearl oyster, which is consistent with previous observations reported by Wang et al. (2001) for pearl oyster and red abalone. The AFM height data was used to accurately measure the nanoroughness of these surfaces, using the root mean square (RMS) of the height. For each type of nacre the RMS was measured at several locations to produce the results shown in Fig. 6. The surface of top shell was found to be significantly rougher ($RMS=16.8\pm2.9$ nm) than pearl oyster ($RMS=7.1\pm2.0$ nm) and red abalone ($RMS=13.0\pm2.5$ nm for pearl oyster). Surface roughness is known to enhance adhesion of adhesives in general (Volinsky et al., 1999), and the higher tablet roughness of top shell may contribute to its superior interfacial toughness compared to the other two species. Red abalone displayed a rougher surface compared to pearl oyster, but its potential effect was suppressed by the detrimental effect of the weak growth lines.

Since the lower toughness of red abalone was associated with the crack propagating along the weak growth line, further comparative fractographic studies were only focused

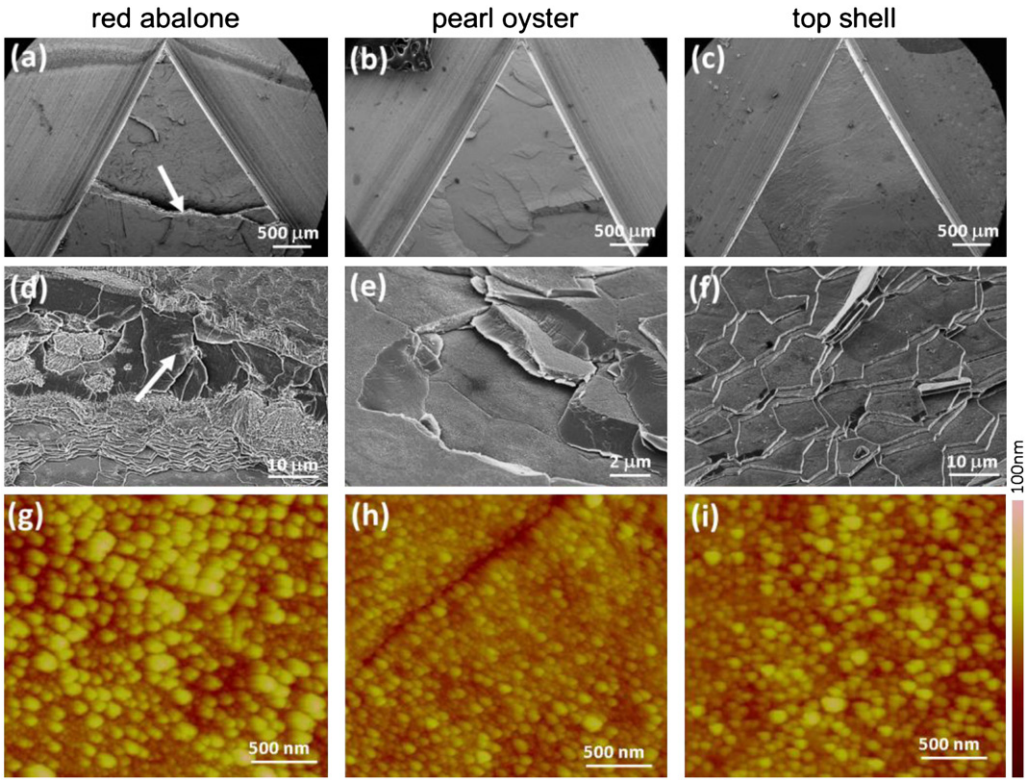

Fig. 5 – (a)–(c) Low magnification SEM micrographs showing the fracture surface of specimens with chevron notch. White arrow in subset (a) indicates a major crack deflection in red abalone. (d)–(f) Typical high magnification SEM micrographs of the fracture surfaces. White arrow in subset (d) shows an instance of a growth line. (g)–(i) Tapping mode AFM height images showing nanoasperities on the tablet surfaces. Left, middle and right column correspond to red abalone, pearl oyster and top shell, respectively.

Please cite this article as: Khayer Dastjerdi, A., et al., The weak interfaces within tough natural composites: Experiments on three types of nacre. Journal of the Mechanical Behavior of Biomedical Materials (2012), http://dx.doi.org/10.1016/j.jmbbm.2012.09.004

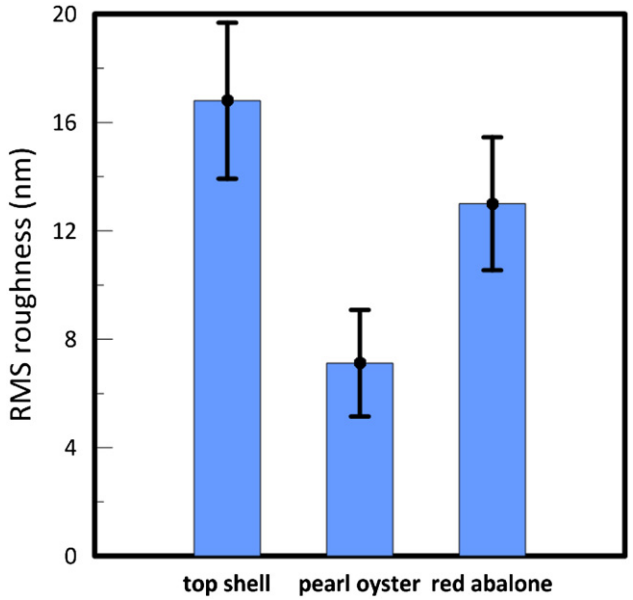

Fig. 6 – RMS roughness of tablets nanograins obtained from AFM height images of the three shells.

on top shell and pearl oyster. AFM images from apposed fracture surfaces were collected in order to identify the mechanisms of crack propagation. The surfaces were not treated with plasma and were imaged shortly after testing. Fig. 7a and b show typical AFM images of apposed faces of a pearl oyster sample. At the microscale, the two fracture faces were highly conformal with the organic material of the junctions between the tablets on one surface imprinted on the opposite face. Higher resolution AFM imaging revealed that most of the organic material remains on one fracture surface, which yields blurry images where asperities can be resolved, but with poor resolution as they lie underneath a continuous layer of organic materials. This was confirmed by a phase image which indicates a relatively homogeneous surface in terms of mechanical properties. Meanwhile, the opposite fracture surface display only remnants of the organic material, located around the exposed mineral asperities. The phase images display a strong contrast as a result of the large difference in material properties between mineral and organic materials. Repeated over several areas of the fracture surface, these observations show that the interface in pearl oyster delaminates through an "adhesive" type of failure (i.e. decohesion of the organic from the mineral surface). Interestingly, adhesive failure invariably occurred along the interface between the organic material and the younger tablets (i.e. the layer of the tablets which is closer to the mantle, Fig. 7b), showing that the organic glue has a stronger binding to the aragonite tablets which were mineralized earlier. The microscopy techniques were also used to characterize the interfacial fracture in top shell (Fig. 7c). In this case we observed a very different failure mechanism. High magnification AFM images show that the organic material is more evenly divided between the two fracture surfaces. The tips of the mineral asperities are protruded through the organic mask covering the fracture surfaces. The interfaces have therefore failed following a mixed mode of "cohesive" and "adhesive" failure (Fig. 7d). The more meandering crack path in the case of top shell may be another factor explaining its superior interfacial toughness compared to the other types of nacre.

4. Tensile tests on isolated organic layers

Finally, the mechanical properties of the organic material itself were measured for all the three types of nacre by performing tensile tests on demineralized samples. Five 20 mm long rectangular tensile specimens from each type of nacre were cut using a precision diamond saw with their long axis being parallel to the inner surface of the shells. The cross section of all the samples was $2.5 \times 3.5\ mm^2$ in average. Two ends of the specimens were then embedded in EpoThin epoxy (two-part Epoxy, Buehler, Lake Bluff, IL, USA) such that approximately 10 mm of the middle of the prisms remained exposed, following a preparation similar to Bezares et al. (2010). The specimens, partially covered by epoxy, were left in ambient temperature for 24 h to be cured. The prepared specimens were then demineralized by immersing in an aqueous solution of 0.5 M ethylene-diamine-tetra-acetic acid (EDTA) for 10 days. After demineralization, the samples were transferred to the miniature loading stage. The samples were clamped through the two rigid epoxy-embedded ends. Tensile tests were performed in a displacement control condition with 10 μm/s pulling rate. During the tests, specimens were kept in a hydrated condition. In order to compute stresses an effective cross sectional area was used, computed by multiplying the apparent cross section of the demineralized sample by 0.05 (the volume concentration of the organic material in nacre). Typical stress–strain curves obtained from tensile tests on the organic matrix of the three nacres are presented in Fig. 8a. The organic matrices displayed a relatively low modulus ($E = 25$–100 MPa) and strength (0.6–1.5 MPa) but high extensibility (2–12% strain). Fig. 8b shows typical failure patterns of the organic phase observed for each case. In red abalone, growth lines played a crucial role since they are thick regions of organic material which are not dissolved in EDTA and withstand a notable portion of the applied stress. As a result, the organic materials from red abalone appeared to be the stiffest ($E = 136$ MPa). In-situ observation of failure process showed that failure first starts with delamination of mesolayers, and then completes with successive failure of each mesolayer in a direction relatively normal to the growth line (Fig. 8b). Pearl oyster and top shell displayed lower moduli ($E = 25$–30 MPa) with an initial toe region probably associated with straightening of the layers. The layers failed progressively at a stress of 0.6–1 MPa, to yield a failure strain of 6–12%. The high strength and low failure strain in the case of red abalone can be attributed to its higher content of stiff chitin fibers compared to that in the two other cases (Bezares et al., 2010). In contrast to red abalone, pearl oyster revealed lower tensile strength accompanied by higher elongation (Fig. 8c), with a failure mechanism displaying a "lock-and-key" feature (Fig. 8b). Top shell, however, showed superior mechanical properties by displaying the highest combination of strength and elongation.

Please cite this article as: Khayer Dastjerdi, A., et al., The weak interfaces within tough natural composites: Experiments on three types of nacre. Journal of the Mechanical Behavior of Biomedical Materials (2012), http://dx.doi.org/10.1016/j.jmbbm.2012.09.004

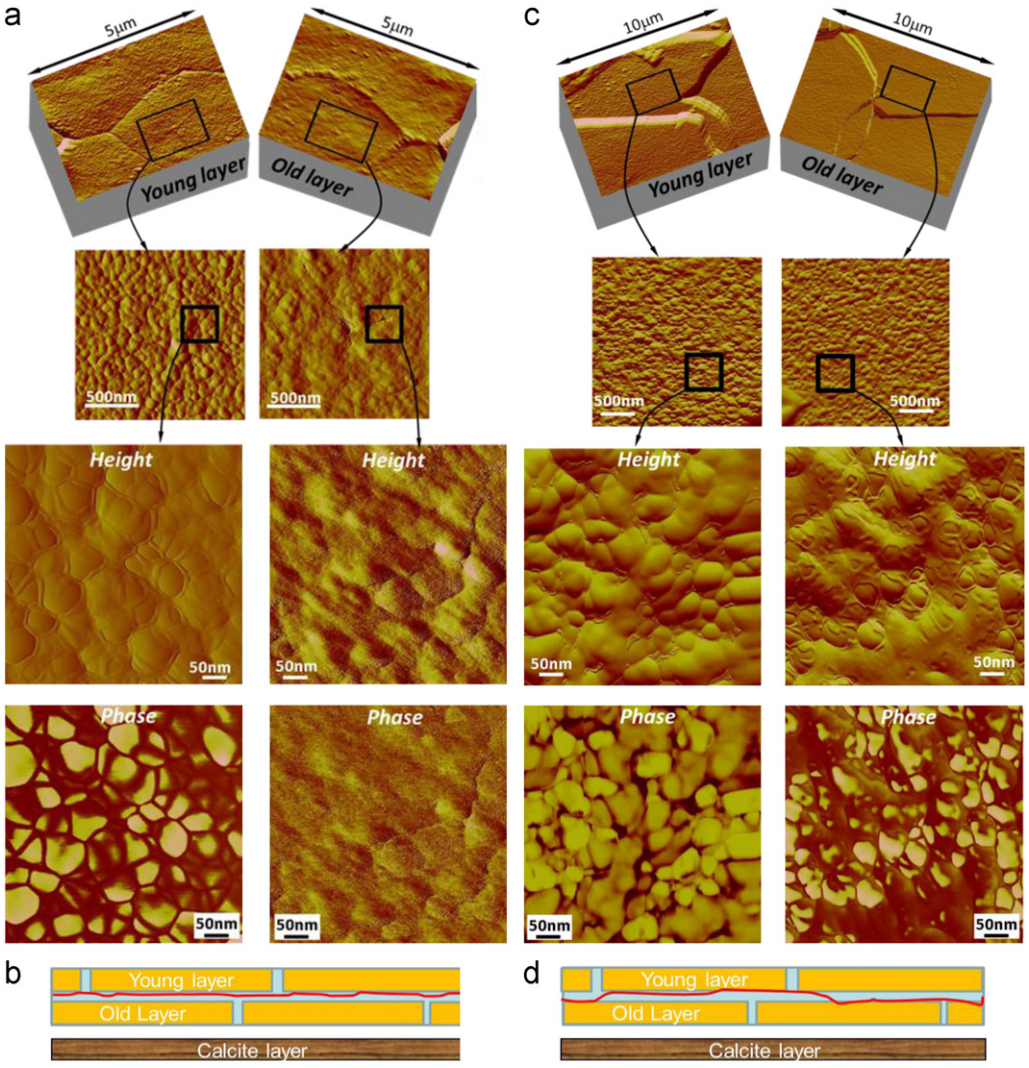

Fig. 7 – Atomic force micrographs of opposed tablets in (a) pearl oyster and (b) top shell along with a schematic illustration of failure mechanism occurring at the interface of the shells, respectively (c and d). Red line in the schematics represents the crack propagation patterns in the two nacre interfaces. (For interpretation of the references to colour in this figure legend, the reader is referred to the web version of this article.)

Failure occurred perpendicular to the loading direction in this case (Fig. 8b).

5. Conclusions

High performance hard biological tissues such as bone, shells, teeth or glass sponge spicules contain a large amount of minerals in the form of layers, rods, grains or platelets bonded by soft organic materials. Since the mineral phase is essentially linear elastic the toughness, damage tolerance and energy dissipation capabilities of these materials rely on the softer organic interfaces. This work focused on nacre, one of the most impressive biological materials in terms of toughness. While the interfaces in nacre are often perceived as tough adherents for the brittle tablets, we found that the interfaces are actually weak, with toughness ranging from 1 to 5.5 J/m^2, which is similar to the toughness of office tape on glass. Surprisingly, the interfaces were also in the range of the toughness of the brittle mineral tablets. This relatively low toughness is in fact desired since cracks must follow the interfaces to deflect and circumvent the mineral tablets in order to trigger toughening mechanisms. These results highlights the tremendous efficacy of the toughening mechanisms operating in nacre (Barthelat and Rabiei, 2011). In fact, even in the interfacial direction we have shown that the intrinsic toughness of the interface is masked by several toughening mechanisms including crack deflection, crack bridging and even process zone. Recent models show that it is deformability (or ductility) and not strength or toughness which is important for the overall toughness of staggered composites (Zhang et al., 2011). The tensile tests presented here show that indeed, isolated organic materials are not strong but that they can deform up to 10% before failure.

In terms of comparison between nacres we found that the interfaces within top shells have by far the highest apparent toughness, which we explained by extensive crack deflection, crack bridging and process zone toughening. The intrinsic

Please cite this article as: Khayer Dastjerdi, A., et al., The weak interfaces within tough natural composites: Experiments on three types of nacre. Journal of the Mechanical Behavior of Biomedical Materials (2012), http://dx.doi.org/10.1016/j.jmbbm.2012.09.004

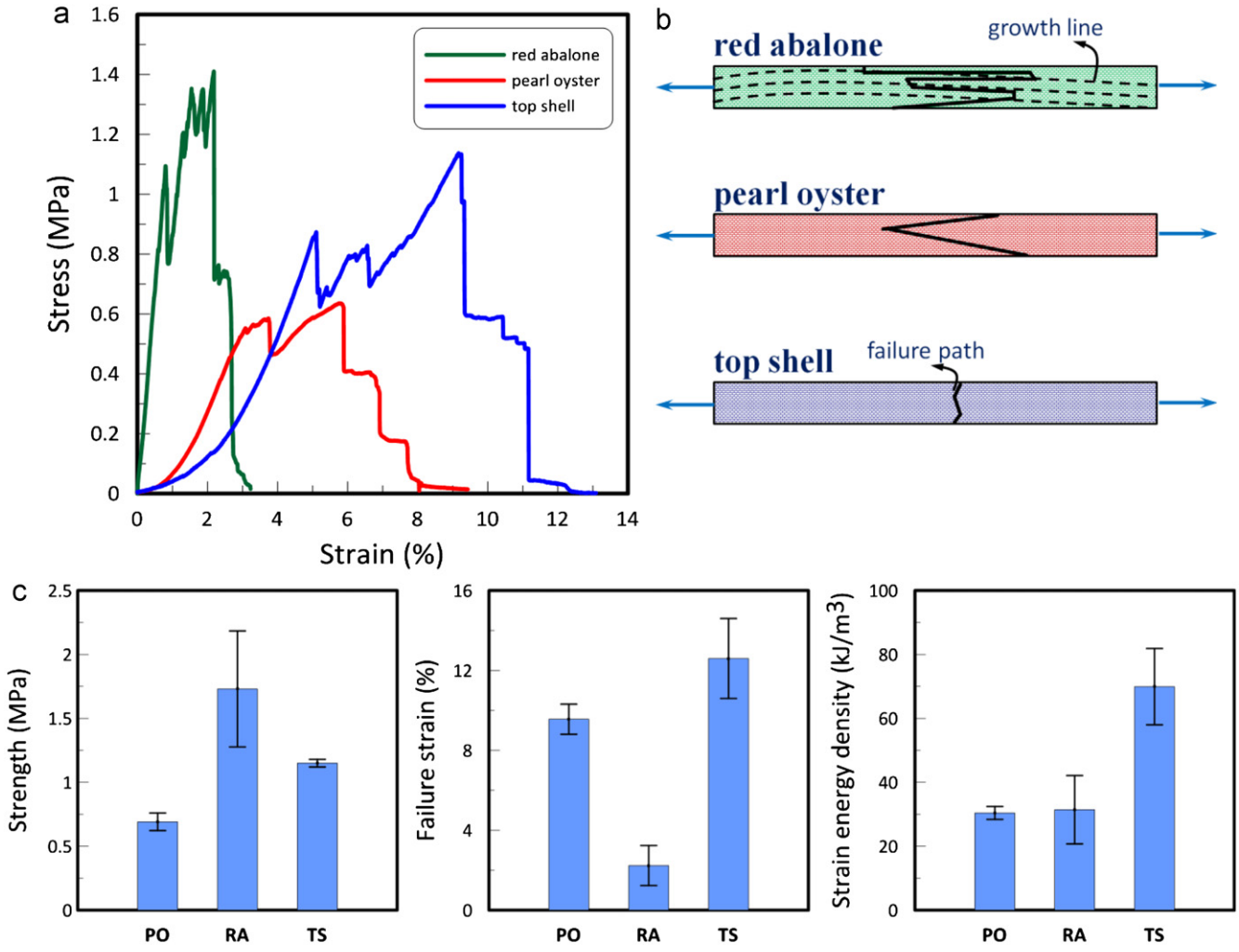

Fig. 8 – (a) Typical stress–strain curves, (b) failure patterns, and (c) measured strength, failure strain and strain energy density for the three demineralized nacres (PO, RA, and TS stand for pearl oyster, read abalone, top shell, respectively).

toughness of the interfaces in top shell was also higher because the adhesion is promoted by higher surface roughness, the organic material can dissipate more energy and the crack is deflected within the interface, with a cohesive/adhesive mixed failure mode. Amongst nacre from red abalone, top shell and pearl oyster the interfacial fracture toughness did not correlate with the across fracture toughness measured previously, because of variations in failure modes and toughening mechanisms (Rabiei et al., 2010). The low interfacial toughness in nacre suggests a more general rule, namely that the nanometers thin interfaces in natural materials, even if made of tough materials, cannot produce high fracture toughness because of their extreme nanoconfinement. This result should greatly facilitate the design and fabrication of nacre-like materials, because the toughness of the interfaces in these engineered materials does not need to be (and should not be) extremely high in order to achieve high toughness at the macroscale. Rather, it is the arrangement and structure of these weaker interfaces in relation to the hard phase which is key to achieving mechanical performance. For example, the hard phase can be arranged in a staggered fashion or over several hierarchy length scales in order to achieve attractive combinations of stiffness, strength and toughness (Gao et al., 2003; Zhang et al., 2011; Sen and Buehler, 2011; Bosia et al., 2010).

Acknowledgment

This work was supported by the Faculty of Engineering at McGill University, the Natural Sciences and Engineering Research Council of Canada, the Canada Foundation for Innovation and the Fonds Québécois de la Recherche sur la Nature et les Technologies. These authors wish to thank Professor Sylvain Coulomb for lending his plasma etching facility.

REFERENCES

Anderson, T.L., 1995. Fracture Mechanics: Fundamentals and Applications, 2nd edition CRC Press.

Barinov, S., 1993. Work-of-fracture determination for brittle materials. Journal of Materials Science Letters 12, 674–676.

Please cite this article as: Khayer Dastjerdi, A., et al., The weak interfaces within tough natural composites: Experiments on three types of nacre. Journal of the Mechanical Behavior of Biomedical Materials (2012), http://dx.doi.org/10.1016/j.jmbbm.2012.09.004

Barthelat, F., 2007. Biomimetics for next generation materials. Philosophical Transactions of the Royal Society a—Mathematical Physical and Engineering Sciences 365, 2907–2919.

Barthelat, F., Rabiei, R., 2011. Toughness amplification in natural composites. Journal of the Mechanics and Physics of Solids 59, 829–840.

Barthelat, F., Tang, H., Zavattieri, P.D., Li, C.M., Espinosa, H.D., 2007a. On the mechanics of mother-of-pearl: a key feature in the material hierarchical structure. Journal of the Mechanics and Physics of Solids 55, 306–337.

Barthelat, F., Tang, H., Zavattieri, P.D., Li, C.M., Espinosa, H.D., 2007b. On the mechanics of mother-of-pearl: a key feature in the material hierarchical structure. Journal of the Mechanics and Physics of Solids 55, 225–444.

Barthelat, F., Zhu, D.J., 2011. A novel biomimetic material duplicating the structure and mechanics of natural nacre. Journal of Materials Research 26, 1203–1215.

Barthelat, F., 2006. The Mechanical Performance of Nacre from Seashells—Superior Toughness Through Microstructural Design. Ph.D. Thesis.

Bezares, J., Asaro, R.J., Hawley, M., 2010. Macromolecular structure of the organic framework of nacre in *Haliotis rufescens*: implications for mechanical response. Journal of Structural Biology 170, 484–500.

Blank, S., Arnoldi, M., Khoshnavaz, S., Treccani, L., Kuntz, M., Mann, K., Grathwohl, G., Fritz, M., 2003. The nacre protein perlucin nucleates growth of calcium carbonate crystals. Journal of Microscopy 212, 280–291.

Bosia, F., Buehler, M.J., Pugno, N.M., 2010. Hierarchical simulations for the design of supertough nanofibers inspired by spider silk. Physical Review E 82, 056103.

Broz, M.E., Cook, R.F., Whitney, D.L., 2006. Microhardness, toughness, and modulus of Mohs scale minerals. American Mineralogist 91, 135–142.

Buehler, M.J., Xu, Z., 2010. Mind the helical crack. Nature 464, 42–43.

Currey, J.D., 1977. Mechanical-properties of mother of pearl in tension. Proceedings of the Royal Society of London Series B—Biological Sciences 196, 443–463.

Dastjerdi, A.K., Pagano, M., Kaartinen, M., Mckee, M., Barthelat, F., 2012. Cohesive behavior of soft biological adhesives: experiments and modeling. Acta Biomaterialia 8, 3349.

Deville, S., Saiz, E., Nalla, R.K., Tomsia, A.P., 2006. Freezing as a path to build complex composites. Science 311, 515–518.

Erasmus, J., 1994. Internal shell structure and growth lines in the shell of the abalone, *Haliotis midae*. Journal of Shellfish Research 13, 493.

Espinosa, H.D., Rim, J.E., Barthelat, F., Buehler, M.J., 2009. Merger of structure and material in nacre and bone—perspectives on de novo biomimetic materials. Progress in Materials Science 54, 1059–1100.

Fantner, G.E., Oroudjev, E., Schitter, G., Golde, L.S., Thurner, P., Finch, M.M., Turner, P., Gutsmann, T., Morse, D.E., Hansma, H., Hansma, P.K., 2006. Sacrificial bonds and hidden length: unraveling molecular mesostructures in tough materials. Biophysical Journal 90, 1411–1418.

Fratzl, P., 2007. Nature's hierarchical materials. Progress in Materials Science 52, 1263.

Fratzl, P., Burgert, I., Gupta, H.S., 2004. On the role of interface polymers for the mechanics of natural polymeric composites. Physical Chemistry Chemical Physics 6, 5575–5579.

Gao, H.J., 2006. Application of fracture mechanics concepts to hierarchical biomechanics of bone and bone-like materials. International Journal of Fracture 138, 101–137.

Gao, H.J., Ji, B.H., Jager, I.L., Arzt, E., Fratzl, P., 2003. Materials become insensitive to flaws at nanoscale: lessons from nature. Proceedings of the National Academy of Sciences of the United States of America 100, 5597–5600.

Hansma, P.K., 2005. Sacrificial bonds in the interfibrillar matrix of bone. Journal of Musculoskeletal & Neuronal Interactions 5, 313.

Imbeni, V., Kruzic, J.J., Marshall, G.W., Marshall, S.J., Ritchie, R.O., 2005. The dentin–enamel junction and the fracture of human teeth. Nature Materials 4, 229–232.

Jackson, A.P., Vincent, J.F.V., Turner, R.M., 1988. The mechanical design of nacre. Proceedings of the Royal Society of London 234, 415–440.

Jäger, I., Fratzl, P., 2000. Mineralized collagen fibrils: a mechanical model with a staggered arrangement of mineral particles. Biophysical Journal 79, 1737–1746.

Koester, K.J., Ager, J.W., Ritchie, R.O., 2008. The true toughness of human cortical bone measured with realistically short cracks. Nature Materials 7, 672–677.

Kotha, S., Li, Y., Guzelsu, N., 2001. Micromechanical model of nacre tested in tension. Journal of Materials Science 36, 2001–2007.

Kruzic, J., Nalla, R.K., Kinney, J.H., Ritchie, R.O., 2003. Crack blunting, crack bridging and resistance-curve fracture mechanics in dentin: effect of hydration. Biomaterials 24, 5209–5221.

Kuhn-Spearing, L., Kessler, H., Chateau, E., Ballarini, R., Heuer, A., Spearing, S., 1996. Fracture mechanisms of the *Strombus gigas* conch shell: implications for the design of brittle laminates. Journal of Materials Science 31, 6583–6594.

Launey, M.E., Buehler, M.J., Ritchie, R.O., 2010. On the mechanistic origins of toughness in bone. Annual Review of Materials Research 40, 25–53.

Lin, A., Meyers, M.A., 2005. Growth and structure in abalone shell. Materials Science and Engineering: A 390, 27–41.

Mayer, G., Sarikaya, M., 2002. Rigid biological composite materials: structural examples for biomimetic design. Experimental Mechanics 42, 395–403.

Meyers, M., Lim, C., Li, A., Hairul Nizam, B., Tan, E., Seki, Y., Mckittrick, J., 2009. The role of organic intertile layer in abalone nacre. Materials Science and Engineering: C 29, 2398–2410.

Meyers, M., Lin, A., Chen, P.-Y., Muyco, J., 2008. Mechanical strength of abalone nacre: role of the soft organic layer. Journal of the Mechanical Behavior of Biomedical Materials 1, 76–85.

Ming-Yuan, H., Hutchinson, J.W., 1989. Crack deflection at an interface between dissimilar elastic materials. International Journal of Solids and Structures 25, 1053–1067.

Munch, E., Launey, M.E., Alsem, D.H., Saiz, E., Tomsia, A.P., Ritchie, R.O., 2008. Tough, bio-inspired hybrid materials. Science 322, 1516.

Nalla, R.K., Kinney, J.H., Ritchie, R.O., 2003. Mechanistic fracture criteria for the failure of human cortical bone. Nature Materials 2, 164–168.

Rabiei, R., Bekah, S., Barthelat, F., 2010. Failure mode transition in nacre and bone-like materials. Acta Biomaterialia 6, 4081–4089.

Ritchie, R.O., 1999. Mechanisms of fatigue-crack propagation in ductile and brittle solids. International Journal of Fracture 100, 55.

Rousseau, M., Lopez, E., Stempfle, P., Brendle, M., Franke, L., Guette, A., Naslain, R., Bourrat, X., 2005. Multiscale structure of sheet nacre. Biomaterials 26, 6254–6262.

Sarikaya, M., Aksay, I.A. (Eds.), 1995. Biomimetics, Design and Processing of Materials. Woodbury, AIP Press, New York.

Sarikaya, M., Fong, H., Sunderland, N., Flinn, B.D., Mayer, G., 2001. Biomimetic model of a sponge-spicular optical fiber—mechanical properties and structure. Journal of Materials Research 16, 1420–1428.

Schäffer, T.E., Ionescu-Zanetti, C., Proksch, R., Fritz, M., Walters, D.A., Almqvist, N., Zaremba, C.M., Belcher, A.M., Smith, B.L., Stucky, G.D., 1997. Does abalone nacre form by heteroepitaxial

Please cite this article as: Khayer Dastjerdi, A., et al., The weak interfaces within tough natural composites: Experiments on three types of nacre. Journal of the Mechanical Behavior of Biomedical Materials (2012), http://dx.doi.org/10.1016/j.jmbbm.2012.09.004

nucleation or by growth through mineral bridges?. Chemistry of Materials 9, 1731–1740.

Sen, D., Buehler, M.J., 2011. Structural Hierarchies Define Toughness and Defect-tolerance Despite Simple and Mechanically Inferior Brittle Building Blocks. Scientific Reports, 1.

Smith, B.L., Schaeffer, T.E., Viani, M., Thompson, J.B., Frederick, N.A., Kindt, J., Belcher, A., Stucky, G.D., Morse, D.E., Hansma, P.K., 1999a. Molecular mechanistic origin of the toughness of natural adhesives, fibres and composites. Nature (London) 399, 761–763.

Smith, B.L., Schaffer, T.E., Viani, M., Thompson, J.B., Frederick, N.A., Kindt, J., Belcher, A., Stucky, G.D., Morse, D.E., Hansma, P.K., 1999b. Molecular mechanistic origin of the toughness of natural adhesives, fibres and composites. Nature 399, 761–763.

Song, F., Bai, Y., 2003. Effects of nanostructures on the fracture strength of the interfaces in nacre. Journal of Materials Research 18, 1741–1744.

Thurner, P.J., 2007. High-speed photography of compressed human trabecular bone correlates whitening to microscopic damage. Engineering Fracture Mechanics 74, 1928.

Tvergaard, V., Hutchinson, J.W., 1996. On the toughness of ductile adhesive joints. Journal of the Mechanics and Physics of Solids 44, 789–800.

Volinsky, A., Nelson, J., Gerberich, W., 1999. Macroscopic modelling of fine line adhesion tests. Materials Research Society, 297–302.

Wang, R., Gupta, H.S., 2011. Deformation and fracture mechanisms of bone and nacre. Annual Review of Materials Research 41, 41–73.

Wang, R.Z., Suo, Z., Evans, A.G., Yao, N., Aksay, I.A., 2001. Deformation mechanisms in nacre. Journal of Materials Research 16, 2485–2493.

Weiner, S., Traub, W., Parker, S., 1984. Macromolecules in mollusc shells and their functions in biomineralization [and Discussion]. Philosophical Transactions of the Royal Society of London B, Biological Sciences 304, 425–434.

Xu, Z.H., Li, X., 2011. Deformation strengthening of biopolymer in nacre. Advanced Functional Materials.

Yourdkhani, M., Pasini, D., Barthelat, F., 2011. Multiscale mechanics and optimization of gastropod shells. Journal of Bionic Engineering 8, 357–368.

Zhang, Z., Zhang, Y.W., Gao, H., 2011. On optimal hierarchy of load-bearing biological materials. Proceedings of the Royal Society B: Biological Sciences 278, 519–525.

Zioupos, P., Hansen, U., Currey, J.D., 2008. Microcracking damage and the fracture process in relation to strain rate in human cortical bone tensile failure. Journal of Biomechanics 41, 2932–2939.

Please cite this article as: Khayer Dastjerdi, A., et al., The weak interfaces within tough natural composites: Experiments on three types of nacre. Journal of the Mechanical Behavior of Biomedical Materials (2012), http://dx.doi.org/10.1016/j.jmbbm.2012.09.004